ANZIAM J. 57(2016), 461–481
doi:10.1017/S1446181116000067

A WAVELET COLLOCATION SCHEME FOR SOLVING SOME OPTIMAL PATH PLANNING PROBLEMS

MARZIYEH MORTEZAEE✉ [1] and ALIREZA NAZEMI[1]

(Received 23 December, 2014; accepted 22 September, 2015; first published online 12 May 2016)

Abstract

We consider an approximation scheme using Haar wavelets for solving optimal path planning problems. The problem is first expressed as an optimal control problem. A computational method based on Haar wavelets in the time domain is then proposed for solving the obtained optimal control problem. A Haar wavelets integral operational matrix and a direct collocation method are used to find an approximate optimal trajectory of the original problem. Numerical results are also presented for several examples to demonstrate the applicability and efficiency of the proposed method.

2010 *Mathematics subject classification*: primary 49J15; secondary 65T60, 90C30.

Keywords and phrases: optimal path planning problems, approximation, rationalized Haar functions, nonlinear programming.

1. Introduction

Finding an optimal path planning is one of the most applicable problems, especially in the robot industry, the military and recently in surgery planning [1]. Latombe [11] has gathered novel methods for path planning in the presence of obstacles. Wang et al. [28] have considered two novel approaches: constrained optimization and semi-infinite constrained optimization for unmanned underwater vehicle path planning. Borzabadi et al. [1] have presented a new approach based on measure theory for finding the approximate optimal path in the presence of obstacles. Zamirian et al. [29] have proposed an applicable method for solving the shortest path problem. There are many other methods for solving the optimal path planning problem (for example, see [12, 13]).

Orthogonal functions such as Haar wavelets [7, 9], Walsh functions [4, 23], block pulse functions [15, 18, 22], Laguerre polynomials [8], Legendre polynomials [3], Chebyshev functions [6] and Fourier series [26], which are often used to represent

[1]Department of Mathematics, School of Mathematical Sciences, Shahrood University of Technology, P.O. Box 3619995161-316, Shahrood, Iran; e-mail: mortezaee91@gmail.com, nazemi20042003@yahoo.com.

arbitrary time functions, have frequently been used to deal with various problems of dynamical systems. The main advantage of this approach is that it reduces the difficulties involved in solving problems described by differential equations, such as the analysis of linear time-invariant systems, time-varying systems, model reduction, optimal control and system identification, to the solution of a system of algebraic equations. Thus, the solution, identification and optimization procedures are either greatly reduced or much simplified. The available sets of orthogonal functions can be divided into three classes: piecewise-constant basis functions such as Haar wavelets, Walsh functions and block pulse functions; orthogonal polynomials such as Laguerre, Legendre and Chebyshev polynomials; and sine–cosine functions in Fourier series [16]. Among them, wavelet theory is a relatively new area in mathematical research [2]. It has been applied to a wide range of engineering disciplines, such as signal processing, pattern recognition, industrial chemical reactors and computer graphics. Recently, attempts have been made to use wavelet theory to solve surface integral equations [25], improve the finite-difference time-domain method [10], solve linear differential equations and nonlinear partial differential equations [20, 21], optimal control problems [5] and model nonlinear semiconductor devices [19].

Motivated by the above discussion, in this paper we consider a particular approximation scheme based on Haar wavelets which can be used to solve optimal path planning problems. First, we consider the problem as an optimization problem, and then we convert it to an optimal control problem by defining some artificial control functions. We assume that the control variables and derivatives of the state variables in the optimal control problem may be expressed in the form of Haar wavelets and unknown coefficients. The state variables can be calculated by using the Haar operational integration matrix. Therefore, all variables in the nonlinear system of equations are expressed as a series of the Haar family and its operational matrix. Finally, the task of finding the unknown parameters that optimize the designated performance while satisfying all constraints of the obtained nonlinear programming problems is performed by the nonlinear programming problems. To demonstrate the applicability of the proposed collocation method, we consider several examples of the optimal path planning problems in Section 5.

2. Problem statement and transformation

A general form of an optimal path planning for a rigid and free-flying object $\mathscr{A}$, which is considered as a point, can be considered as the following optimization problem:

$$\text{minimize} \qquad I(q(t), \dot{q}(t)) = \int_0^T F_0(t, q(t), \dot{q}(t))\, dt, \tag{2.1}$$

subject to

$$\varphi_i(t, q(t), \dot{q}(t)) > 0, \quad i = 1, 2, \ldots, s, \ t \in [0, T], \tag{2.2}$$

$$q(0) = q_{\text{init}}, \quad q(T) = q_{\text{goal}}, \tag{2.3}$$

https://doi.org/10.1017/S1446181116000067 Published online by Cambridge University Press

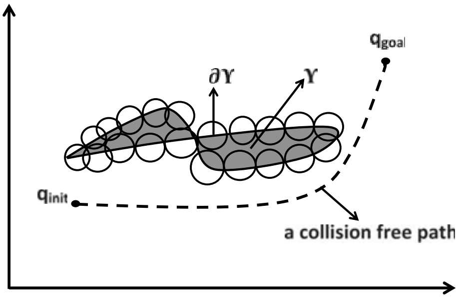

FIGURE 1. Obstacle Υ and its boundary that is covered by circles.

where F_0 is a continuous differentiable function, q is a configuration of space–time $\mathscr{C}$, considered as the position of the object $\mathscr{A}$, I is a functional which represents some geometrical properties of the motion such as the length of the path and the ith inequality in (2.2) is equivalent to the image complement of the ith obstacle $\mathscr{B}_i(t)$ in $\mathscr{C}$ [11], that is, the complement of

$$\mathscr{C}\mathscr{B}_i(t) = \{q \mid \mathscr{A}(q) \cap \mathscr{B}_i(t) \neq \emptyset\} \quad \text{for all } t \in [0, T],$$

where $\mathscr{A}(q)$ is a subset of the workspace occupied by the object $\mathscr{A}$ at configuration q.

We emphasize that in our examples all the stationary or moving obstacles are considered as r_i-radius circles or spheres, $i = 1, 2, \ldots, s$, in plane or space, respectively. For example, in plane if we assume that the ith obstacle at the moment τ is a noncircle geometrical shape, such as $\Upsilon_i = \mathscr{B}_i(\tau)$, and with compact boundary $\partial\Upsilon_i$, then one can cover $\partial\Upsilon_i$ by a finite number of circles, such as C_l, $l = 1, 2, \ldots, L$, such that $C_l \subseteq \mathscr{C}\mathscr{B}_i(\tau)$, $l = 1, 2, \ldots, L$ (see Figure 1). Thus, we can substitute the number of L conditions in our optimization problem instead of the obstacle $\mathscr{B}_i(\tau)$. Now define the artificial control function $u(\cdot)$ as

$$\dot{q}(t) = u(t).$$

The following mix-constrained optimal control problem represents the optimization problem (2.1)–(2.3):

$$\text{minimize} \qquad I(q(t), u(t)) = \int_0^T F_0(t, q(t), u(t))\, dt, \tag{2.4}$$

subject to

$$\dot{q}(t) = u(t), \tag{2.5}$$

$$\varphi_i(t, q(t), u(t)) > 0, \qquad i = 1, 2, \ldots, s, \ t \in [0, T], \tag{2.6}$$

$$q(0) = q_{\text{init}}, \qquad q(T) = q_{\text{goal}}. \tag{2.7}$$

The time transformation $t = T\tau$, $t \in [0, T]$, is introduced in order to use Haar functions defined on $\tau \in [0, 1]$ (see also [14]). Using this transformation, the optimal

https://doi.org/10.1017/S1446181116000067 Published online by Cambridge University Press

control problem of the nonlinear system in (2.5)–(2.7) with performance index in (2.4) is replaced by an optimization problem given by

$$\text{minimize} \qquad I(q(T\tau), u(T\tau)) = \int_0^1 TF_0(T\tau, q(T\tau), u(T\tau))\, d\tau, \tag{2.8}$$

subject to

$$\dot{q}(T\tau) = Tu(T\tau), \tag{2.9}$$

$$\varphi_i(T\tau, q(T\tau), u(T\tau)) > 0, \quad i = 1, 2, \ldots, s, \ \tau \in [0, 1], \tag{2.10}$$

$$q(0) = q_{\text{init}}, \quad q(1) = q_{\text{goal}} \quad T > 0. \tag{2.11}$$

Now we assume that

$$\begin{cases} y(\tau) = q(T\tau), \\ v(\tau) = u(T\tau). \end{cases}$$

Thus, the problem of the nonlinear system (2.9)–(2.11) with the performance index in (2.8) is replaced by one as follows:

$$\text{minimize} \qquad I(y(\tau), v(\tau)) = \int_0^1 TF_0(T\tau, y(\tau), v(\tau))\, d\tau, \tag{2.12}$$

subject to

$$\dot{y}(\tau) = Tv(\tau), \tag{2.13}$$

$$\varphi_i(T\tau, y(\tau), v(\tau)) > 0, \quad i = 1, 2, \ldots, s, \ \tau \in [0, 1], \tag{2.14}$$

$$y(0) = q_{\text{init}}, \quad y(1) = q_{\text{goal}}, \quad T > 0.$$

3. Haar wavelets

3.1. Rationalized Haar functions The rationalized Haar (RH) functions $RH(r, \tau)$, $r = 1, 2, \ldots,$ can be defined on the interval $[0, 1)$ (see, for example, [17]) by

$$RH(r, \tau) = \begin{cases} 1, & J_1 \leqslant \tau < J_{1/2}, \\ -1, & J_{1/2} \leqslant \tau < J_0, \\ 0 & \text{otherwise}, \end{cases}$$

where

$$J_u = \frac{j - u}{2^i}, \quad u = 0, \frac{1}{2}, 1$$

and

$$r = 2^i + j - 1, \quad i = 0, 1, 2, 3, \ldots, \quad j = 1, 2, 3, \ldots, 2^i.$$

For $i = j = 0$, $RH(0, \tau)$ is given by

$$RH(0, \tau) = 1, \quad 0 \leqslant \tau < 1.$$

The orthogonality property is given by

$$\int_0^1 RH(r, \tau) RH(v, \tau)\, d\tau = \begin{cases} 2^{-i}, & r = v, \\ 0, & r \neq v, \end{cases}$$

https://doi.org/10.1017/S1446181116000067 Published online by Cambridge University Press

where

$$\nu = 2^n + m - 1, \quad n = 0, 1, 2, 3, \ldots, \quad m = 1, 2, 3, \ldots, 2^n.$$

Note that the set of RH functions is a complete orthogonal set in the Hilbert space $L^2[0,1]$. Thus, we can expand any function in this space in terms of RH functions.

3.2. Function approximation A function $\mathcal{F}(\tau) \in L^2[0,1]$ may be expanded as an infinite series of RH functions as

$$\mathcal{F}(\tau) = \sum_{r=0}^{\infty} a_r RH(r,\tau), \tag{3.1}$$

where the coefficients a_r are given by

$$a_r = 2^i \int_0^1 \mathcal{F}(\tau) RH(r,\tau)\, d\tau, \quad r = 0, 1, 2, \ldots.$$

If we let $i = 0, 1, 2, \ldots, \alpha$, then the infinite series in (3.1) is truncated up to its first K terms as

$$\mathcal{F}(\tau) \simeq \sum_{r=0}^{K-1} a_r RH(r,\tau) = A^T \Phi(\tau), \tag{3.2}$$

where

$$K = 2^{\alpha+1}, \quad \alpha = 0, 1, 2, 3, \ldots.$$

The vector of unknown coefficients A and $\Phi(\tau)$ are defined as

$$A = [a_0, a_1, \ldots, a_{K-1}]^T,$$
$$\Phi(\tau) = [\phi_0(\tau), \phi_1(\tau), \ldots, \phi_{K-1}(\tau)]^T$$

and

$$\phi_r(\tau) = RH(r,\tau), \quad r = 0, 1, 2, \ldots, K-1.$$

If we set all the collocation points τ_l at the middle of each respective wavelet, then τ_l is defined as

$$\tau_l = \frac{l - 0.5}{K}, \quad l = 1, 2, \ldots, K.$$

With these collocation points, the function is discretized over a series of equally spaced nodes. The vector $\Phi(\tau)$ can also be determined at these collocation points. Let the Haar matrix $\hat{\Phi}_{K\times K}$ be the combination of $\Phi(\tau)$ at all the collocation points. Thus,

$$\hat{\Phi}_{K\times K} = [\Phi(\tau_1), \Phi(\tau_2), \ldots, \Phi(\tau_K)]. \tag{3.3}$$

Using (3.2) and (3.3) yields

$$[\mathcal{F}(\tau_1), \mathcal{F}(\tau_2), \ldots, \mathcal{F}(\tau_K)] = A^T \hat{\Phi}_{K\times K} \tag{3.4}$$

https://doi.org/10.1017/S1446181116000067 Published online by Cambridge University Press

and, from (3.4),

$$A^T = [\mathcal{F}(\tau_1), \mathcal{F}(\tau_2), \ldots, \mathcal{F}(\tau_K)]\hat{\Phi}^{-1}_{K\times K},$$

where

$$\hat{\Phi}^{-1}_{K\times K} = \left(\frac{1}{K}\right)\hat{\Phi}^T_{K\times K}\,\mathrm{diag}\left(1, 1, 2, 2, \underbrace{2^2, \ldots, 2^2}_{2^2}, \underbrace{2^3, \ldots, 2^3}_{2^3}, \ldots, \underbrace{\frac{K}{2}, \ldots, \frac{K}{2}}_{K/2}\right). \tag{3.5}$$

Therefore, the function $\mathcal{F}(\tau)$ is approximated as

$$\mathcal{F}(\tau_l) \approx A^T_{1\times K}\hat{\Phi}_{K\times K}, \quad l = 1, 2, \ldots, K,$$

which approximates the function $\mathcal{F}(\tau)$ with minimum mean integral square error

$$\varepsilon = \int_0^1 (\mathcal{F}(\tau) - A^T\Phi(\tau))^2\, d\tau.$$

Obviously, ε decreases when K gets larger and converges to zero when K approaches infinity.

3.3. Operational matrix of integration In the solution of optimal control problems, we always need to deal with equations involving differentiation and integration. If the system function is expressed in Haar wavelets, the integration or differentiation operation of Haar series cannot be avoided. The differentiation of step waves will generate pulse signals which are difficult to handle, while the integration of step waves will result in constant-slope functions which can be calculated by the following equation:

$$\int_0^\tau \Phi(\tau')\, d\tau' \simeq P\,\Phi(\tau),$$

where

$$P = P_{K\times K} = \frac{1}{2K}\begin{bmatrix} 2KP_{K/2\times K/2} & -\hat{\Phi}_{K/2\times K/2} \\ \hat{\Phi}^{-1}_{K/2\times K/2} & 0 \end{bmatrix}. \tag{3.6}$$

This has been derived by Razzaghi and Ordokhani [24] with $\hat{\Phi}_{1\times 1} = [1]$ and $P_{1\times 1} = [1/2]$. Here $\hat{\Phi}_{K/2\times K/2}$ and $\hat{\Phi}^{-1}_{K/2\times K/2}$ can be obtained from (3.3) and (3.5), respectively. The integration of the cross product of the two RH vectors is derived as

$$\int_0^1 \Phi(\tau)\Phi^T(\tau)\, d\tau = D,$$

where

$$D = \mathrm{diag}\left(1, 1, \frac{1}{2}, \frac{1}{2}, \underbrace{\frac{1}{2^2}, \ldots, \frac{1}{2^2}}_{2^2}, \ldots, \underbrace{\frac{1}{2^\alpha}, \ldots, \frac{1}{2^\alpha}}_{2^\alpha}\right) \tag{3.7}$$

is the diagonal matrix.

https://doi.org/10.1017/S1446181116000067 Published online by Cambridge University Press

4. Direct collocation

4.1. Haar discretization method In the discussion of Haar wavelets, we have already addressed how to approximate a function via Haar wavelets and its corresponding operational integration matrix. We are going to apply this methodology in optimal control problems so that Haar discretization is used in direct collocation [5]. Thus, the continuous solution to a problem will be represented by state and control variables in terms of Haar series and its operational matrix to satisfy the differential equations. The standard interval considered here is denoted as $\tau \in [0, 1)$ with collocation points

$$\tau_l = \frac{l - 0.5}{K}, \quad l = 1, 2, \ldots, K,$$

where K is the number of nodes used in the discretization and also the maximum wavelet index number. Note that the magnitude of K is a power of 2, so that the number of collocation points is also increasing by the same power. All the collocation points are equally distributed over the entire time interval $[0, 1)$ with $1/K$ as the time distance to adjacent nodes. We assume that the derivatives of the state variables $\dot{y}(\tau)$ and control variables $v(\tau)$ can be approximated by Haar wavelets with K collocation points, that is,

$$\dot{y}(\tau) \approx C_y^T \Phi(\tau),$$
$$v(\tau) \approx C_v^T \Phi(\tau),$$

where

$$C_y^T = [C_{y1}, C_{y2}, \ldots, C_{yK}], \quad C_v^T = [C_{v1}, C_{v2}, \ldots, C_{vK}].$$

Using the operational integration matrix P defined in (3.6), the state variables $y(\tau)$ can be expressed as

$$y(\tau) = \int_0^\tau \dot{y}(\tau')\, d\tau' + y_0 = \int_0^\tau C_y^T \Phi(\tau')\, d\tau' + y_0 = C_y^T P\, \Phi(\tau) + y_0.$$

As stated in (3.3), the expansion of the matrix $\Phi(\tau)$ at the K collocation points will yield the $K \times K$ Haar matrix $\hat{\Phi}$. It follows that

$$\dot{y}(\tau_l) = C_y^T \Phi(\tau_l), \quad v(\tau_l) = C_v^T \Phi(\tau_l), \quad y(\tau_l) = C_y^T P\, \Phi(\tau_l) + y_0, \quad l = 1, \ldots, K. \tag{4.1}$$

From the above expression, we can evaluate the variables at any collocation point by using the product of its coefficient vector and the corresponding column vector in the Haar matrix.

4.2. Nonlinear programming When the Haar collocation method is applied in the optimal control problems, the nonlinear programming variables can be set as the unknown coefficient vectors of the derivatives of the state variables and control variables, that is,

$$y = [C_{y1}, C_{y2}, \ldots, C_{yK}, C_{v1}, C_{v2}, \ldots, C_{vK}].$$

https://doi.org/10.1017/S1446181116000067 Published online by Cambridge University Press

The performance index in (2.12) is then restated as

$$I = \int_0^1 T F_0(T\tau, (C_y^T P\Phi(\tau) + y_0), C_v^T \Phi(\tau))\, d\tau.$$

Since the Haar wavelets are expected to be constant steps at each time interval, the above equation can be simplified to

$$I = \frac{T}{K} \sum_{l=1}^{K} F_0(T\tau_l, (C_y^T P\Phi(\tau_l) + y_0), C_v^T \Phi(\tau_l)),$$

with path constraints (2.14)

$$\varphi_i(T\tau_l, (C_y^T P\Phi(\tau_l) + y_0), C_v^T \Phi(\tau_l)) > 0, \quad i = 1, 2, \ldots, s, \quad l = 1, 2, \ldots, K.$$

Substituting $\dot{y}, v$ and y in (2.13) with the Haar wavelet expressions (4.1) separately yields

$$C_y^T \Phi(\tau_l) = T C_v^T \Phi(\tau_l), \quad l = 1, 2, \ldots, K.$$

The system equation constraints and path constraints are all treated as nonlinear constraints in a nonlinear programming solver. The boundary constraints need more attention. Since the first and last collocation points are not set as the initial and final times, the initial and final state variables are calculated according to

$$y_0 = y(\tau_1) - \frac{\dot{y}(\tau_1)}{2K}, \quad y_1 = y(\tau_K) + \frac{\dot{y}(\tau_K)}{2K}.$$

In this way, the optimal control problems are transformed into nonlinear programming problems in a structured form, which are solved by GAMS software [27].

5. Numerical examples

In this section, we apply our proposed approach to some optimal path planning problems. We consider the moving object as a point in the examples. Also, we assume that the obstacles have circle forms in $\mathbb{R}^2$ and sphere forms in $\mathbb{R}^3$ with known equations.

EXAMPLE 5.1. Consider the problem of finding shortest path planning in the plane in the presence of five stationary circle obstacles. We consider this problem as an optimization problem. The configuration space is the Euclidean space $\mathbb{R}^2$. Now the problem is as follows:

$$\text{minimize} \int_0^1 \sqrt{(\dot{q}_1(t))^2 + (\dot{q}_2(t))^2}\, dt,$$

subject to

$$\begin{aligned} &\varphi_i(t, q(t), \dot{q}(t)) > 0, \quad i = 1, 2, \ldots, 5, \\ &q_1(0) = q_2(0) = 0, \qquad q_1(1) = q_2(1) = 1, \end{aligned}$$

https://doi.org/10.1017/S1446181116000067 Published online by Cambridge University Press

TABLE 1. Results for Example 5.1.

Wavelet with	Cost function
$K = 32$	1.4521711169
$K = 64$	1.4532694177
$K = 128$	1.4534062522
$K = 256$	1.4533974591

where $\varphi_i(t, q(t), \dot{q}(t)) = (x_1(t) - \alpha_i)^2 + (x_2(t) - \beta_i)^2 - r_i^2$. As in Section 2, we transform the problem to the following optimal control problem:

$$\begin{aligned}
&\text{minimize } \int_0^1 \sqrt{(u_1(t))^2 + (u_2(t))^2}\, dt,\\
&\text{subject to}\\
&\qquad \dot{q}_1(t) = u_1(t),\\
&\qquad \dot{q}_2(t) = u_2(t),\\
&\qquad \varphi_i(t, q(t), u(t)) > 0, \quad i = 1, 2, \ldots, 5,\\
&\qquad q_1(0) = q_2(0) = 0, \qquad q_1(1) = q_2(1) = 1
\end{aligned}$$

and $\varphi_i(t, q(t), u(t)) = (q_1(t) - \alpha_i)^2 + (q_2(t) - \beta_i)^2 - r_i^2$. The centre of obstacles (circles) and their radii considered are

$$\begin{aligned}
(\alpha_1, \beta_1) &= (0.5, 0.5), & r_1 &= \tfrac{1}{8},\\
(\alpha_2, \beta_2) &= (0.7, 0.85), & r_2 &= \tfrac{1}{8},\\
(\alpha_3, \beta_3) &= (0.2, 0.2), & r_3 &= \tfrac{1}{8},\\
(\alpha_4, \beta_4) &= (0.3, 0.8), & r_4 &= \tfrac{1}{8},\\
(\alpha_5, \beta_5) &= (0.75, 0.2), & r_5 &= \tfrac{1}{8}.
\end{aligned}$$

We summarize the results in Table 1 with different values of K. In Figures 2 and 3, one can see the approximate optimal trajectory and optimal artificial control constructed by Haar wavelets.

We impose some changes in the place of obstacles as follows:

$$\begin{aligned}
(\alpha_2, \beta_2) &= (0.7, 0.8), & r_2 &= \tfrac{1}{8},\\
(\alpha_3, \beta_3) &= (0.45, 0.2), & r_3 &= \tfrac{1}{8},\\
(\alpha_4, \beta_4) &= (0.3, 0.7), & r_4 &= \tfrac{1}{8}.
\end{aligned}$$

Results for different values of K are given in Table 2. The approximate optimal trajectory and optimal artificial control are shown in Figures 4 and 5.

EXAMPLE 5.2. In this example, we consider an optimal path planning with moving obstacles. Again, the converted optimal control problem corresponding to the original

https://doi.org/10.1017/S1446181116000067 Published online by Cambridge University Press

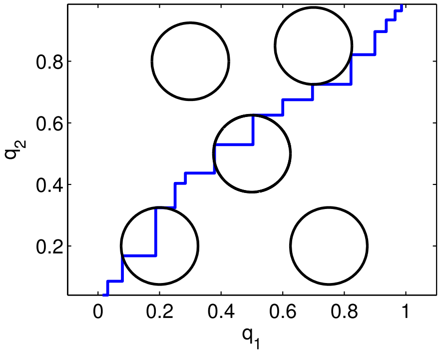

(a) Approximate optimal trajectory obtained for $K = 16$.

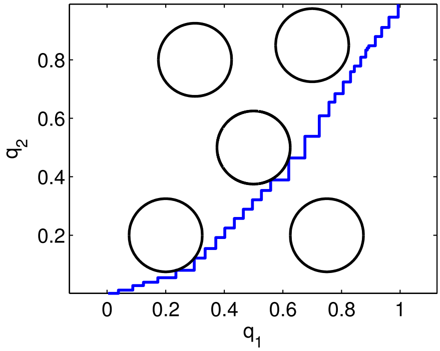

(b) Approximate optimal trajectory obtained for $K = 32$.

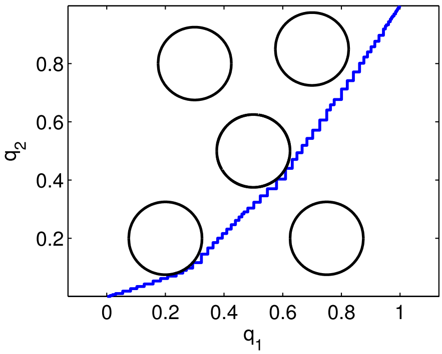

(c) Approximate optimal trajectory obtained for $K = 64$.

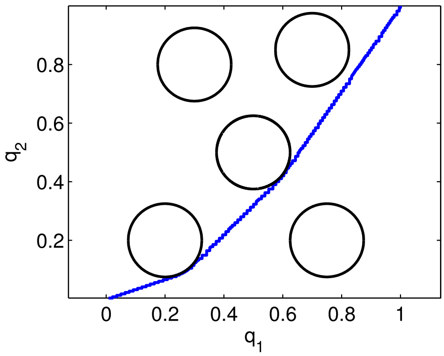

(d) Approximate optimal trajectory obtained for $K = 128$.

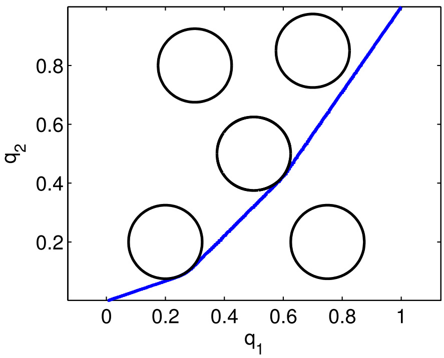

(e) Approximate optimal trajectory obtained for $K = 256$.

FIGURE 2. Approximate optimal trajectory obtained for Example 5.1.

https://doi.org/10.1017/S1446181116000067 Published online by Cambridge University Press

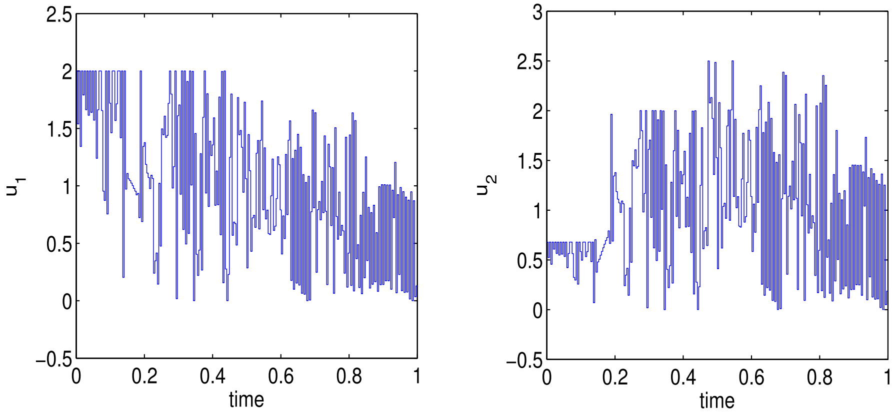

FIGURE 3. Approximate optimal artificial control obtained for $K = 256$ in Example 5.1.

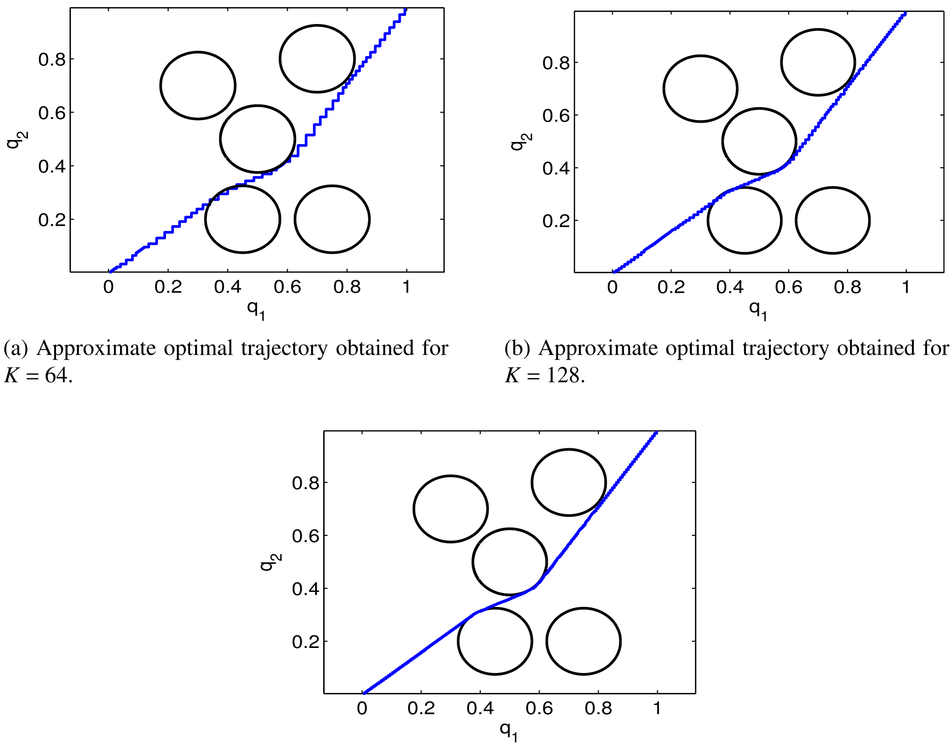

(a) Approximate optimal trajectory obtained for $K = 64$.

(b) Approximate optimal trajectory obtained for $K = 128$.

(c) Approximate optimal trajectory obtained for $K = 256$.

FIGURE 4. Approximate optimal trajectory obtained for Example 5.1 (after imposing some changes).

https://doi.org/10.1017/S1446181116000067 Published online by Cambridge University Press

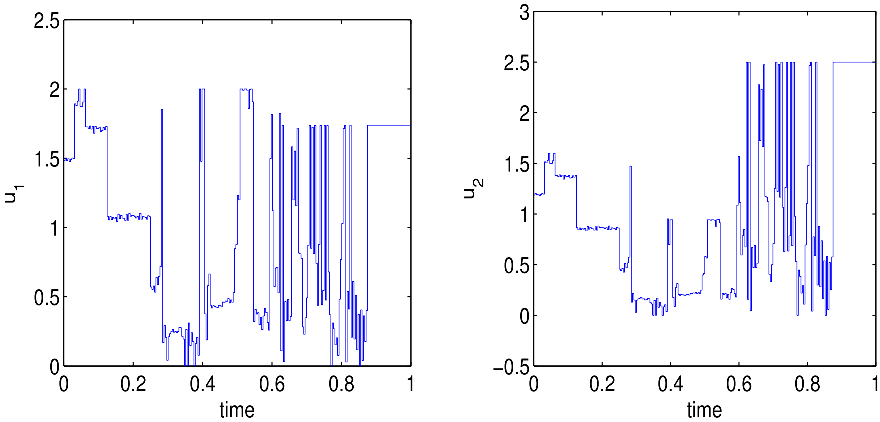

FIGURE 5. Approximate optimal artificial control obtained for $K = 256$ in Example 5.1 (after imposing some changes).

TABLE 2. Results for Example 5.1 (after imposing some changes).

Wavelet with	Cost function
$K = 64$	1.4400222633
$K = 128$	1.4400767341
$K = 256$	1.4400624679

problem is as follows:

$$\begin{aligned}
&\text{minimize} \int_0^1 \sqrt{(u_1(t))^2 + (u_2(t))^2}\,dt,\\
&\text{subject to}\\
&\qquad \dot{q}_1(t) = u_1(t), \quad \dot{q}_2(t) = u_2(t),\\
&\qquad \varphi_i(t, q(t), u(t)) > 0, \quad i = 1, 2, \ldots, s,\\
&\qquad q_1(0) = q_2(0) = 0, \qquad q_1(1) = q_2(1) = 1
\end{aligned}$$

and $\varphi_i(t, q(t), u(t)) = (q_1(t) - \alpha_i)^2 + (q_2(t) - \beta_i)^2 - r_i^2$.

We consider the problem in two cases. First, only one moving obstacle is considered as

$$\varphi(t, q(t), u(t)) = (q_1(t) - \alpha)^2 + (q_2(t) - \beta)^2 - r^2,$$

where

$$\begin{cases} \alpha(t) = t, \\ \beta(t) = 0.5 \end{cases}$$

https://doi.org/10.1017/S1446181116000067 Published online by Cambridge University Press

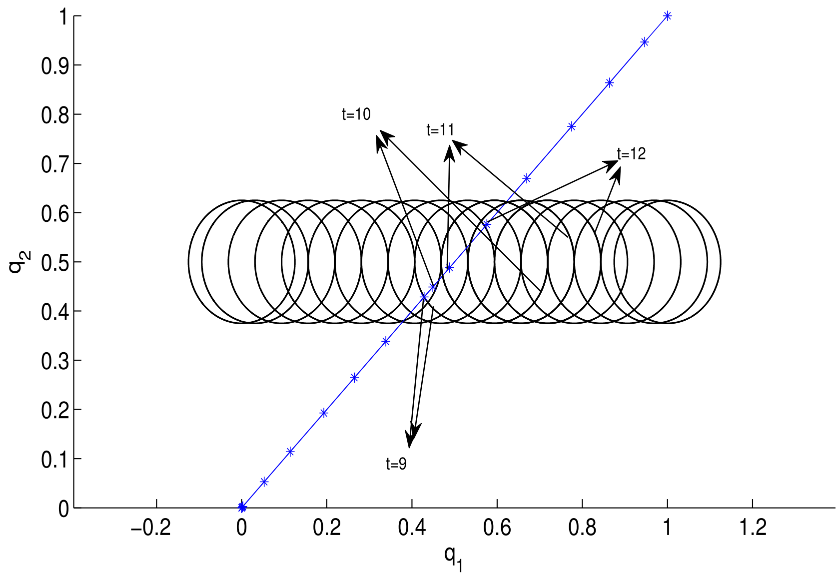

(a) Approximate optimal trajectory obtained for $K = 16$. The position of obstacles and object in the ith unit of time is shown by $t = i$.

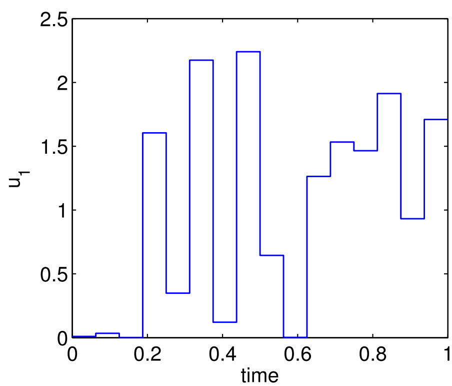

(b) Approximate optimal artificial control u_1 obtained for $K = 16$.

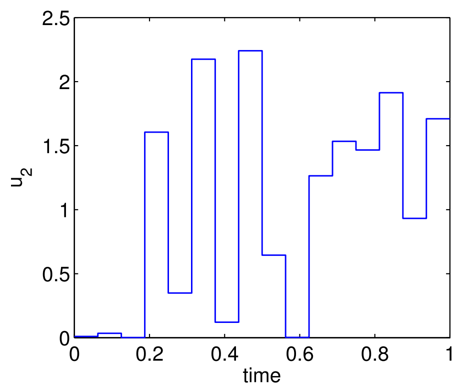

(c) Approximate optimal artificial control u_2 obtained for $K = 16$.

FIGURE 6. Approximate optimal trajectory and artificial control obtained for Example 5.2 (in the first case).

and $r = 1/8$. The position of approximate optimal trajectory and moving obstacles are shown in Figure 6.

In the second case, we consider two moving obstacles

$$\varphi_i(t, q(t), u(t)) = (q_1(t) - \alpha_i)^2 + (q_2(t) - \beta_i)^2 - r_i^2, \quad i = 1, 2,$$

https://doi.org/10.1017/S1446181116000067 Published online by Cambridge University Press

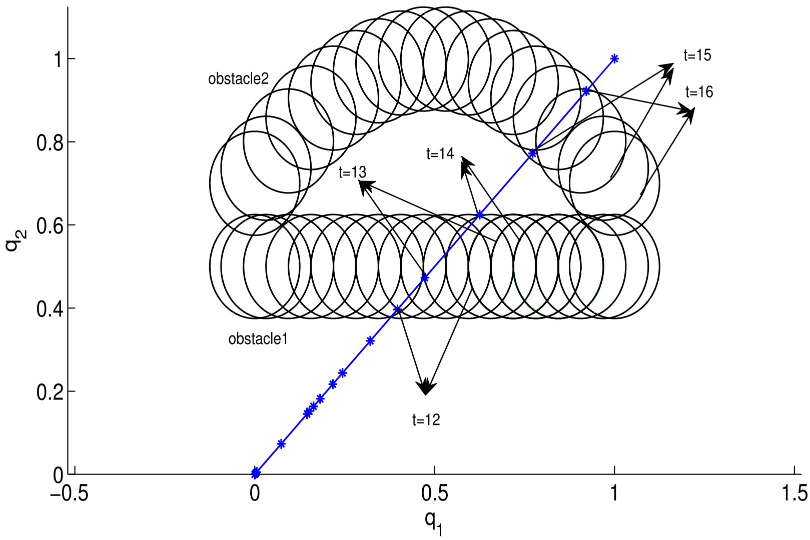

(a) Approximate optimal trajectory obtained for $K = 16$. The position of obstacles and the object in ith unit of time is shown by $t = i$.

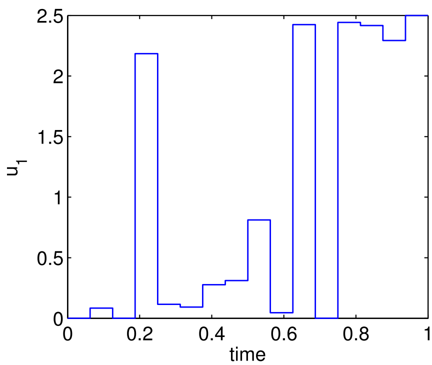

(b) Approximate optimal artificial control u_1 obtained for $K = 16$.

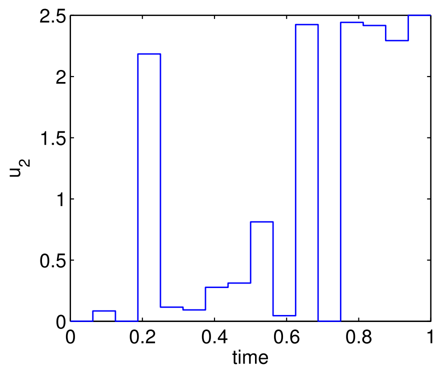

(c) Approximate optimal artificial control u_2 obtained for $K = 16$.

FIGURE 7. Approximate optimal trajectory and artificial control obtained for Example 5.2 (in the second case).

where

$$\begin{cases} \alpha_1(t) = t, \\ \beta_1(t) = 0.5 \end{cases} \quad \text{and} \quad \begin{cases} \alpha_2(t) = t, \\ \beta_2(t) = -1.2t^2 + 1.2t + 0.7 \end{cases}$$

and $r_1 = r_2 = 1/8$. The position of moving obstacles and approximate optimal trajectory are shown in Figure 7.

https://doi.org/10.1017/S1446181116000067 Published online by Cambridge University Press

EXAMPLE 5.3. Now we consider a shortest path planning problem in $\mathbb{R}^3$, where we convert the problem to the following optimal control problem:

$$
\begin{aligned}
&\text{minimize} \int_0^1 \sqrt{(u_1(t))^2 + (u_2(t))^2 + (u_3(t))^2}\, dt,\\
&\text{subject to}\\
&\qquad \dot{q}_1(t) = u_1(t),\\
&\qquad \dot{q}_2(t) = u_2(t),\\
&\qquad \dot{q}_3(t) = u_3(t),\\
&\qquad \varphi_i(t, q(t), u(t)) > 0, \quad i = 1, 2, \ldots, s,\\
&\qquad q_1(0) = q_2(0) = q_3(0) = 0, \quad q_1(1) = q_2(1) = q_3(1) = 1
\end{aligned}
$$

and $\varphi_i(t, q(t), \dot{u}(t)) = (q_1(t) - \alpha_i)^2 + (q_2(t) - \beta_i)^2 + (q_3(t) - \gamma_i)^2 - r_i^2$.

We solve the problem in two cases. In the first case, we consider only one obstacle (sphere) with $(\alpha, \beta, \gamma) = (0.5, 0.5, 0.5)$ and radius $r = 1/6$. In Figure 8, the approximate optimal trajectory and optimal artificial control are shown.

In the second case, we restrict the free space by adding four obstacles in the workspace. The centre and radius of obstacles (spheres) considered are

$$
\begin{aligned}
(\alpha_1, \beta_1, \gamma_1) &= (0.5, 0.5, 0.5), & r_1 &= \tfrac{1}{6},\\
(\alpha_2, \beta_2, \gamma_2) &= (0.3, 0.3, 0.1), & r_2 &= \tfrac{1}{5},\\
(\alpha_3, \beta_3, \gamma_3) &= (0.8, 0.2, 0.6), & r_3 &= \tfrac{1}{5},\\
(\alpha_4, \beta_4, \gamma_4) &= (0.2, 0.2, 0.8), & r_4 &= \tfrac{1}{5},\\
(\alpha_5, \beta_5, \gamma_5) &= (0.2, 0.8, 0.4), & r_5 &= \tfrac{1}{5}.
\end{aligned}
$$

In Figure 9, the approximate optimal trajectory and optimal artificial control are shown.

EXAMPLE 5.4. We consider an optimal path planning with moving obstacles in $\mathbb{R}^3$. Again, the converted optimal control problem corresponding to the original problem is as follows:

$$
\begin{aligned}
&\text{minimize} \int_0^1 \sqrt{(u_1(t))^2 + (u_2(t))^2 + (u_3(t))^2}\, dt,\\
&\text{subject to}\\
&\qquad \dot{q}_1(t) = u_1(t),\\
&\qquad \dot{q}_2(t) = u_2(t),\\
&\qquad \dot{q}_3(t) = u_3(t),\\
&\qquad \varphi_i(t, q(t), u(t)) > 0, \quad i = 1, 2, \ldots, s,\\
&\qquad q_1(0) = q_2(0) = q_3(0) = 0, \qquad q_1(1) = q_2(1) = q_3(1) = 1.
\end{aligned}
$$

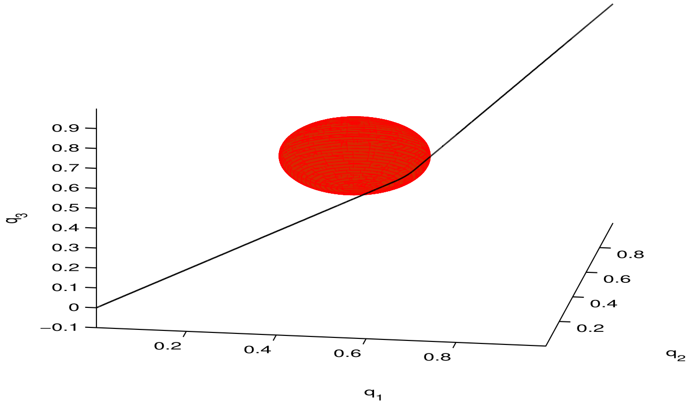

(a) Approximate optimal trajectory obtained for $K = 1024$.

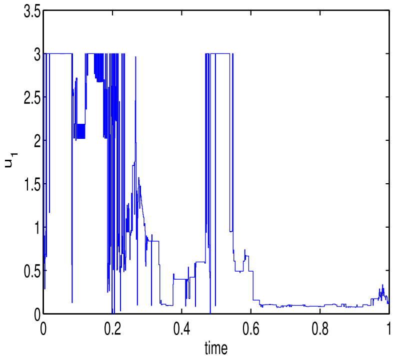

(b) Approximate optimal artificial control u_1 obtained for $K = 1024$.

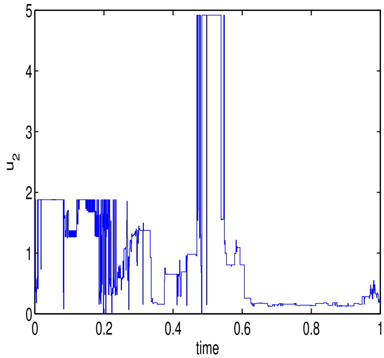

(c) Approximate optimal artificial control u_2 obtained for $K = 1024$.

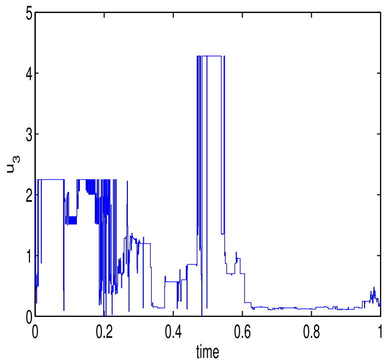

(d) Approximate optimal artificial control u_3 obtained for $K = 1024$.

FIGURE 8. Approximate optimal trajectory and artificial control obtained for Example 5.3 (in the first case).

https://doi.org/10.1017/S1446181116000067 Published online by Cambridge University Press

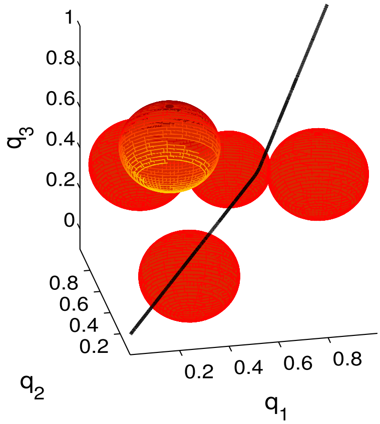

(a) Approximate optimal trajectory obtained for $K = 1024$.

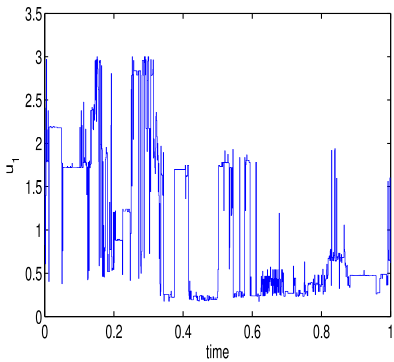

(b) Approximate optimal artificial control u_1 obtained for $K = 1024$.

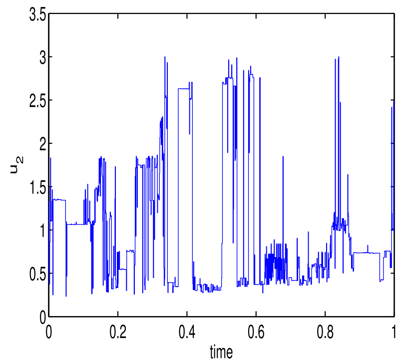

(c) Approximate optimal artificial control u_2 obtained for $K = 1024$.

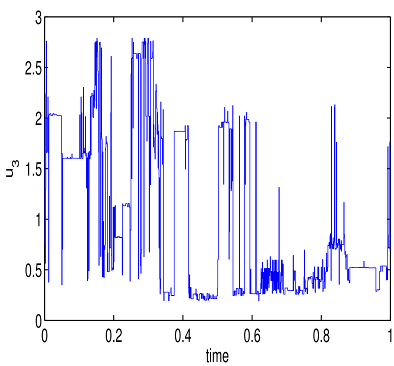

(d) Approximate optimal artificial control u_3 obtained for $K = 1024$.

FIGURE 9. Approximate optimal trajectory and artificial control obtained for Example 5.3 (in the second case).

https://doi.org/10.1017/S1446181116000067 Published online by Cambridge University Press

We consider two moving obstacles

$$\varphi_i(t, q(t), u(t)) = (q_1(t) - \alpha_i)^2 + (q_2(t) - \beta_i)^2 + (q_3(t) - \gamma_i)^2 - r_i^2, \quad i = 1, 2,$$

where

$$\begin{cases} \alpha_1(t) = t, \\ \beta_1(t) = 0.5, \\ \gamma_1(t) = 0.5 \end{cases} \quad \text{and} \quad \begin{cases} \alpha_2(t) = t, \\ \beta_2(t) = -1.2t^2 + 1.2t + 0.5, \\ \gamma_2(t) = -1.2t^2 + 1.2t + 0.7 \end{cases}$$

and $r_1 = r_2 = 1/10$. In Figure 10, the approximate optimal trajectory and optimal artificial control constructed by Haar wavelets are shown.

To conclude this section, we answer a natural question: "Are there advantages of the proposed collocation method compared to the existing ones?" To answer this, we summarize what we have observed from numerical experiments and theoretical results as follows.

- One of the main advantages of using Haar wavelets is that the matrices $\hat{\Phi}_{K\times K}, \hat{\Phi}^{-1}_{K\times K}$ and D introduced in (3.3), (3.5) and (3.7) have large numbers of zero elements and they are sparse; hence, the present method is very attractive and reduces the CPU time and computer memory at the same time as keeping the accuracy of the solution.
- The simple implementation of Haar wavelet-based optimal control in real applications is interesting.
- Haar functions are also notable for their rapid convergence for the expansion of functions, and this capability makes them very useful in regard to the Haar function theory.
- The proposed method also produces results similar to other collocation methods for the continuous optimal control problem.
- The proposed orthogonal collocation method leads to a rapid convergence as the number of collocation points increases.

6. Conclusion

Approximate solutions to optimal path planning problems were obtained by a combined algorithm of parameters and function optimization. To this end, and to use the Haar wavelet functions, a suitable transformation was used to obtain a related problem. On the basis of the approximation of dynamical systems and the performance index into Haar series, an efficient and accurate method was then applied for solving optimal path planning problems. Several illustrative examples were included to demonstrate the validity and applicability of the proposed method.

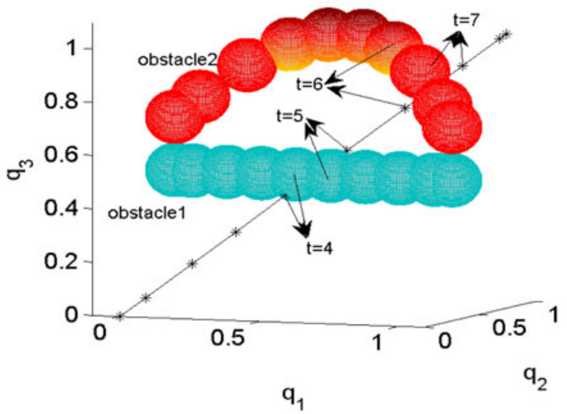

(a) Approximate optimal trajectory obtained for $K = 8$. The position of obstacles and object in the ith unit of time is shown by $t = i$.

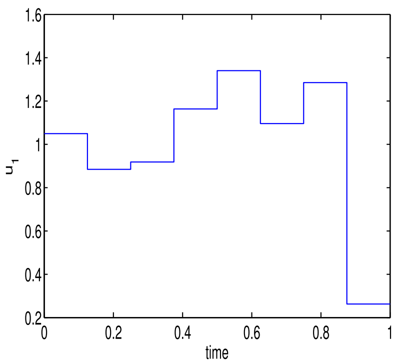

(b) Approximate optimal artificial control u_1 obtained for $K = 8$.

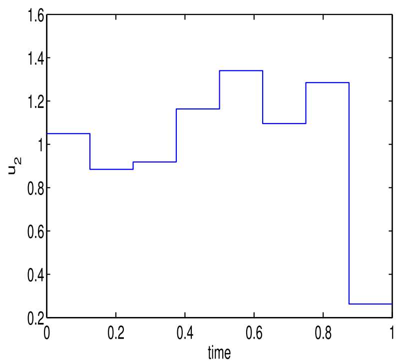

(c) Approximate optimal artificial control u_2 obtained for $K = 8$.

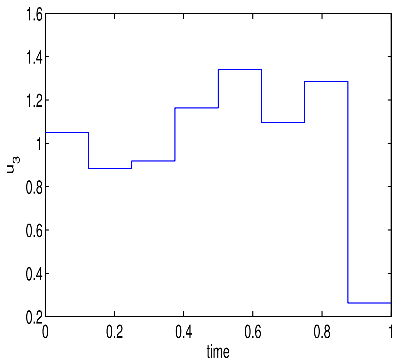

(d) Approximate optimal artificial control u_3 obtained for $K = 8$.

FIGURE 10. Approximate optimal trajectory and artificial control obtained for Example 5.4.

https://doi.org/10.1017/S1446181116000067 Published online by Cambridge University Press

References

[1] A. H. Borzabadi, A. V. Kamyad, M. H. Farahi and H. H. Mehne, “Solving some optimal path planning problems using an approach based on measure theory”, *Appl. Math. Comput.* **170** (2005) 1418–1435; doi:10.1016/j.amc.2005.01.035.

[2] C. S Burrus, R. A. Gopinath and H. Guo, *Introduction to wavelets and wavelet transforms: a primer* (Prentice Hall, Upper Saddle River, NJ, 1998).

[3] R. Y. Chang and M. L. Wang, “Legendre polynomials approximation to dynamic linear state equations with initial or boundary value conditions”, *Internat. J. Control* **40** (1984) 215–232; doi:10.1080/00207178408933269.

[4] C. F. Chen and C. H. Hsiao, “A state-space approach to Walsh series solution of linear systems”, *Internat. J. Systems Sci.* **6** (1975) 833–858; doi:10.1080/00207727508941868.

[5] R. Dai and J. E. Cochran, “Wavelet collocation method for optimal control problems”, *J. Optim. Theory Appl.* **143** (2009) 265–278; doi:10.1007/s10957-009-9565-9.

[6] I. R. Horng and J. H. Chou, “Analysis, parameter estimation and optimal control of time-delay systems via Chebyshev series”, *Internat. J. Control* **41** (1985) 1221–1234; doi:10.1080/0020718508961193.

[7] C. H. Hsiao and W. J. Wang, “State analysis and parameter estimation of bilinear systems via Haar wavelets”, *IEEE Trans. Circuits Syst. I. Fundam. Theor. Appl.* **47** (2000) 246–250; doi:10.1109/81.828579.

[8] C. Hwang and Y. P. Shih, “Laguerre operational matrices for fractional calculus and applications”, *Internat. J. Control* **34** (1981) 577–584; doi:10.1080/00207178108922549.

[9] H. R. Karimi, B. Lohmann, P. Jabehdar Maralani and B. Moshiri, “A computational method for solving optimal control and parameter estimation of linear systems using Haar wavelets”, *Int. J. Comput. Math.* **81** (2004) 1121–1132; doi:10.1080/03057920412331272225.

[10] H. R. Karimi, B. Moshiri, B. Lohmann and P. Jabehdar Maralani, “Haar wavelet-based approach for optimal control of second-order linear systems in time domain”, *J. Dyn. Control Syst.* **11** (2005) 237–252; doi:10.1007/s10883-005-4172-z.

[11] J. C. Latombe, *Robot motion planning* (Kluwer Academic, Norwell, MA, 1991).

[12] B. Li, K. L. Teo, G. H. Zhao and G. R. Duan, “An efficient computational approach to a class of minimax optimal control problems with applications”, *ANZIAM J.* **51** (2009) 162–177; doi:10.1017/S1446181110000040.

[13] B. Li, C. Xu, K. L. Teo and J. Chu, “Time optimal Zermelo’s navigation problem with moving and fixed obstacles”, *Appl. Math. Comput.* **224** (2013) 866–875; doi:10.1016/j.amc.2013.08.092.

[14] C. Liu, R. Loxton and K. L. Teo, “A computational method for solving time-delay optimal control problems with free terminal time”, *Systems Control Lett.* **72** (2014) 53–60; doi:10.1016/j.sysconle.2014.07.001.

[15] H. R. Marzban and M. Razzaghi, “Optimal control of linear delay systems via hybrid of block-pulse and Legendre polynomials”, *J. Franklin Inst.* **341** (2004) 279–293; doi:10.1016/j.jfranklin.2003.12.011.

[16] H. R. Marzban and M. Razzaghi, “Solution of time-varying delay systems by hybrid functions”, *Math. Comput. Simulation* **64** (2004) 597–607; doi:10.1016/j.matcom.2003.10.003.

[17] H. R. Marzban and M. Razzaghi, “Rationalized Haar approach for nonlinear constrained optimal control problems”, *Appl. Math. Model.* **34** (2010) 174–183; doi:10.1016/j.apm.2009.03.036.

[18] S. Mashayekhi, Y. Ordokhani and M. Razzaghi, “Hybrid functions approach for nonlinear constrained optimal control problems”, *Commun. Nonlinear Sci. Numer. Simul.* **17** (2012) 1831–1843; doi:10.1016/j.cnsns.2011.09.008.

[19] T. Nagura, T. Yamazato, M. Katayama, T. Yendo, T. Fujii and H. Okada, “Improved decoding methods of visible light communication system for ITS using LED array and high-speed camera”, in: *Proc. 71st IEEE Vehicular Technology Conference (VTC 2010 Spring), Taipei, Taiwan, 16–19 May 2010*, (IEEE, 2010) 1–5; doi:10.1109/VETECS.2010.5493958.

[20] M. Ohkita and Y. Kobayashi, "An application of rationalized Haar functions to solution of linear differential equations", *IEEE Trans. Circuits Syst. I. Regul. Pap.* **33** (1986) 853–862; doi:10.1109/TCS.1986.1086019.

[21] M. Ohkita and Y. Kobayashi, "An application of rationalized Haar functions to solution of linear partial differential equations", *Math. Comput. Simulation* **30** (1988) 419–428; doi:10.1016/0378-4754(88)90055-9.

[22] G. P. Rao, *Piecewise constant orthogonal functions and their application to systems and control* (Springer, Berlin–Heidelberg, 2003).

[23] M. Razzaghi and J. Nazarzadeh, "Walsh functions", in: *Wiley encyclopedia of electrical and electronics engineering* (1999); doi:10.1002/047134608X.W2465.

[24] M. Razzaghi and Y. Ordokhani, "Solution of differential equations via rationalized Haar functions", *Math. Comput. Simulation* **56** (2001) 235–246; doi:10.1016/S0378-4754(01)00278-6.

[25] M. Razzaghi and Y. Ordokhani, "A rationalized Haar functions method for nonlinear Fredholm–Hammerstein integral equations", *Int. J. Comput. Math.* **79** (2002) 333–343; doi:10.1080/00207160211932.

[26] M. Razzaghi and M. Razzaghi, "Fourier series direct method for variational problems", *Internat. J. Control* **48** (1988) 887–895; doi:10.1080/00207178808906224.

[27] R. E. Rosenthal and A. Brooke, *GAMS: a user's guide* (GAMS Development Corporation, Washington, DC, 2004) www.GAMS.com.

[28] Y. Wang, D. M. Lane and G. J. Falconer, "Two novel approaches for unmanned under water vehicle path planning: constrained optimisation and semi-infinite constrained optimisation", *Robotica* **18** (2000) 123–142; doi:10.1017/S0263574799002015.

[29] M. Zamirian, M. H. Farahi and A. R. Nazemi, "An applicable method for solving the shortest path problems", *Appl. Math. Comput.* **190** (2007) 1479–1486; doi:10.1016/j.amc.2007.02.057.